

---

---

ELECTRODYNAMICS  
AND WAVE PROPAGATION

---

---

# Application of the Method of Extended Boundary Conditions to the Solution of the Problem of Wave Diffraction by Magnetodielectric Scatterers Having a Compound Geometry

D. V. Krysanov<sup>a, \*</sup>, A. G. Kyurkchan<sup>a, b, c</sup>, and S. A. Manenkov<sup>a</sup>

<sup>a</sup>*Moscow Technical University of Communications and Informatics, Moscow, 111024 Russia*

<sup>b</sup>*Kotelnikov Institute of Radio Engineering and Electronics (Fryazino Branch), Russian Academy of Sciences,  
Fryazino, Moscow oblast, 141190 Russia*

<sup>c</sup>*Central Research Communication Institute, Moscow, 111141 Russia*

\*e-mail: dimok1993@mail.ru

Received October 31, 2019; revised October 31, 2019; accepted November 27, 2019

**Abstract**—A technique allowing to model scattering characteristics for bodies of arbitrary geometries is suggested on the basis of the method of extended boundary conditions. The scattering characteristics include those ones, which are averaged over orientation angles. The 2D problem of diffraction of a plane wave by dielectric bodies having a complicated geometry of the cut and, in particular, by bodies similar to fractals is considered. The numerical algorithms of the diffraction problem solution on the basis of the systems of integral equations of the first and second kinds are compared. The correctness of the method is confirmed with the help of the verification of the optical theorem fulfillment for various bodies and by comparing with the calculation results obtained by the modified method of discrete sources.

**DOI:** 10.1134/S1064226920080148

## INTRODUCTION

The problem of wave diffraction by a dielectric body of a complicated geometry is rather actual and it remains to be comparatively little investigated, because its solution is rather complex. The results of modeling the characteristics of wave scattering by dielectric bodies are of important interest, for example, in such fields as the optics of inhomogeneous media, laser defectoscopy, projecting of absorbing coatings, and others [1–3]. At present, a number of analytical and numerical methods are developed for solving these problems. The  $T$ -matrix method [4] and the discrete source method [5] are the most widespread of them. In spite of that, the requirements of modeling diffraction processes increase rather quickly. Therefore, the problem of developing more universal methods of solution of diffraction problems still remains actual. The wide popularity of the  $T$ -matrix method is explained in many respects by the fact that this method can be used to fulfill comparatively easily such an important, for example, in astrophysics, procedure as averaging the characteristics of scattering of a body over its orientation angles measured with respect to the incident plane wave. However, the traditional (classic) variant of the  $T$ -matrix method [4], as some of its recently developed modified variants [5, 6], can be applied to the solution of problems of diffraction by scatterers having an analytical boundary.

The generalization of the  $T$ -matrix method based on the extended boundary condition method (EBCM) for solving the diffraction problem with the Dirichlet boundary condition in the 2D and 3D cases is suggested in works [7, 8]. The 2D case is also considered for the impedance boundary condition [9]. The EBCM idea is to transfer the boundary condition from surface  $S$  of the scatterer to certain auxiliary surface  $S_\delta$  situated outside the scatterer at certain sufficiently small distance  $\delta$  from its boundary. The absence of limitations of restrictions on the scatterer geometry can be declared as the main advantage of the EBCM. This method can be also applied to scatterers having boundary fractures and to thin screens. In addition, the EBCM offers the common approach to the solution of boundary value problems. This approach does not depend on their type, the dimensionality, the geometry of the scatterer surface, and the character of the scattered field. We should also note that, within the framework of the EBCM, the diffraction problem can be reduced to the solution of the system of integral equations (SIEs) of the first or second kind. This approach is impossible, for example, when the problem is solved using the method of surface integral equations.

In this article, we generalize the above technique for the solution of the 2D problem of electromagnetic wave diffraction by a dielectric body. Examples of modeling the characteristics of scattering by bodies

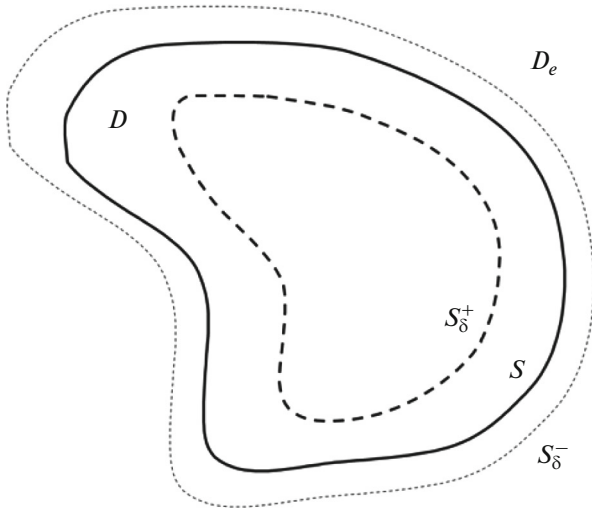


Fig. 1. Geometry of the problem.

with cross-sections of a complex geometry and by bodies similar to fractals are considered. The scattering pattern and the pattern averaged over orientation angles are calculated.

### 1. THE DERIVATION OF THE FUNDAMENTAL RELATIONSHIPS

Assume that primary electromagnetic field  $\vec{E}^0, \vec{H}^0$  is incident on an infinitely long magnetodielectric cylinder with a generatrix parallel to the  $Oz$  axis and directrix  $S$ . The geometry of the problem is shown in Fig. 1. We consider the case of the  $E$  polarization, when the vector of electric field intensity  $\vec{E}$  has only one component  $E_z$  (denoted below as  $U_-$  or  $U_+$ ), which is parallel to the generatrix of the cylindrical body. Then, the following conjugation conditions are valid on the scatterer boundary:

$$U_+|_S = U_-|_S, \quad \frac{\partial U_+}{\partial n}|_S = \kappa \frac{\partial U_-}{\partial n}|_S, \quad (1)$$

where  $U_+$  is the field inside the cylinder;  $U_- = U^0 + U^1$  is the total field outside the body, here,  $U^0$  is the incident field and  $U^1$  is the scattered (secondary) field;  $\partial/\partial n$  denotes the differentiation along the normal, which is external to  $S$ ;  $\kappa = \mu_i/\mu_e$ ; and  $\mu_i$  and  $\mu_e$  are the absolute permeabilities of the media inside and outside the body, respectively. The external medium (where  $D_e = \mathbb{R}^2 \setminus \bar{D}$ ,  $\bar{D} = D \cup S$ , and  $D$  is the region restricted by curve  $S$ ) and the medium inside the cylinder are assumed to be homogeneous, linear, and isotropic. The standard radiation conditions for the scattered field are assumed to be fulfilled at infinity.

We use the following representations for the solution of the Helmholtz equation in regions  $D$  and  $D_e$ , respectively [5]:

$$U_-(\vec{r}) = U^0(\vec{r}) + \int_S \left\{ U_-(\vec{r}') \frac{\partial G_-(\vec{r}, \vec{r}')}{\partial n'} - \frac{\partial U_-(\vec{r}')}{\partial n'} G_-(\vec{r}, \vec{r}') \right\} ds', \quad (2)$$

$$U_+(\vec{r}) = - \int_S \left\{ U_+(\vec{r}') \frac{\partial G_+(\vec{r}, \vec{r}')}{\partial n'} - \frac{\partial U_+(\vec{r}')}{\partial n'} G_+(\vec{r}, \vec{r}') \right\} ds',$$

where  $G_{\pm}(\vec{r}; \vec{r}') = \frac{1}{4i} H_0^{(2)}(k_{\pm}|\vec{r} - \vec{r}'|)$  are the funda-

mental solutions of the scalar Helmholtz equation in  $\mathbb{R}^2$  with the material parameters of media  $D_e$  and  $D$ , respectively, and  $k_+$  and  $k_-$  are the wavenumbers of the medium inside and outside the scatterer. Requiring, according to the EBCM, the fulfillment of conditions (1) on contour  $S_{\delta}^-$  situated in  $\mathbb{R}^2 \setminus \bar{D}$  and on contour  $S_{\delta}^+$  situated in region  $D$  (see Fig. 1), we obtain the following Fredholm SsIEs of the first and second kinds, respectively:

$$\int_S \left\{ U(\vec{r}') \left( \frac{\partial G_-(\vec{r}_-, \vec{r}')}{\partial n'} + \frac{\partial G_+(\vec{r}_+, \vec{r}')}{\partial n'} \right) - \frac{\partial U(\vec{r}')}{\partial n'} (G_-(\vec{r}_-, \vec{r}') + \kappa G_+(\vec{r}_+, \vec{r}')) \right\} ds' = -U^0(\vec{r}_-), \quad (3)$$

$$\int_S \left\{ U(\vec{r}') \left( \frac{\partial^2 G_-(\vec{r}_-, \vec{r}')}{\partial n \partial n'} + \frac{1}{\kappa} \frac{\partial^2 G_+(\vec{r}_+, \vec{r}')}{\partial n \partial n'} \right) - \frac{\partial U(\vec{r}')}{\partial n'} \left( \frac{\partial G_-(\vec{r}_-, \vec{r}')}{\partial n} + \frac{\partial G_+(\vec{r}_+, \vec{r}')}{\partial n} \right) \right\} ds' = -\frac{\partial U^0(\vec{r}_-)}{\partial n},$$

$$U(\vec{r}) = \frac{1}{2} U^0(\vec{r}_-)$$

$$+ \frac{1}{2} \int_S \left\{ U(\vec{r}') \left( \frac{\partial G_-(\vec{r}_-, \vec{r}')}{\partial n'} - \frac{\partial G_+(\vec{r}_+, \vec{r}')}{\partial n'} \right) - \frac{\partial U(\vec{r}')}{\partial n'} (G_-(\vec{r}_-, \vec{r}') - \kappa G_+(\vec{r}_+, \vec{r}')) \right\} ds', \quad (4)$$

$$\frac{\partial U(\vec{r})}{\partial n} = \frac{1}{1 + \kappa} \frac{\partial U^0(\vec{r}_-)}{\partial n} + \frac{1}{1 + \kappa} \times \int_S \left\{ U(\vec{r}') \left( \frac{\partial^2 G_-(\vec{r}_-, \vec{r}')}{\partial n \partial n'} - \frac{\partial^2 G_+(\vec{r}_+, \vec{r}')}{\partial n \partial n'} \right) - \frac{\partial U(\vec{r}')}{\partial n'} \times \left( \frac{\partial G_-(\vec{r}_-, \vec{r}')}{\partial n} - \kappa \frac{\partial G_+(\vec{r}_+, \vec{r}')}{\partial n} \right) \right\} ds',$$

where observation points  $M(\vec{r}_{\pm})$  belong to contours  $S_{\delta}^{\pm}$ ,  $M(\vec{r}) \in S$ , and it is denoted that  $U = U_-$ . Note that most often the contours that are situated at certain sufficiently small distance  $\delta$  away from  $S$  are chosen as  $S_{\delta}^{\pm}$  [5, 10], i.e., equidistant contours are considered. Let the equation of boundary  $S$  be specified in the parametrical form

$$\begin{cases} x = x'(t), \\ y = y'(t), \quad t \in [0, t_{\max}]. \end{cases} \quad (5)$$

Then, the equations of displaced contours  $S_8^\mp$  are written in the following form:

$$\begin{cases} x(t) = x'(t) \pm n_x(t)\delta, \\ y(t) = y'(t) \pm n_y(t)\delta, \end{cases} \quad (6)$$

where  $n_x$  and  $n_y$  are the coordinates of the normal to boundary  $S$  of the body. For the solution of systems (3) and (4), the Krylov–Bogolyubov method is applied. To this end, we write the systems of equations (3) and (4) in the form

$$\begin{aligned} \int_0^{t_{\max}} (K_{11}(t, t')I_1(t') + K_{12}(t, t')I_2(t')) dt' &= b_1(t), \\ \int_0^{t_{\max}} (K_{21}(t, t')I_1(t') + K_{22}(t, t')I_2(t')) dt' &= b_2(t), \end{aligned} \quad (7)$$

$$I_1(t) + \int_0^{t_{\max}} (\tilde{K}_{11}(t, t')I_1(t') + \tilde{K}_{12}(t, t')I_2(t')) dt' = \tilde{b}_1(t), \quad (8)$$

$$I_2(t) + \int_0^{t_{\max}} (\tilde{K}_{21}(t, t')I_1(t') + \tilde{K}_{22}(t, t')I_2(t')) dt' = \tilde{b}_2(t),$$

where the following designations are introduced:

$$\begin{aligned} I_1(t') &= U(\bar{r}'(t')), \quad I_2(t') = \frac{\partial U(\bar{r}'(t'))}{\partial n'}, \\ \xi(t') &= \sqrt{\dot{x}'(t')^2 + \dot{y}'(t')^2}, \\ K_{11} &= \left( \frac{\partial G_-(\bar{r}_-, \bar{r}')}{\partial n'} + \frac{\partial G_+(\bar{r}_+, \bar{r}')}{\partial n'} \right) \xi(t'), \\ K_{12} &= -(G_-(\bar{r}_-, \bar{r}') + \kappa G_+(\bar{r}_+, \bar{r}')) \xi(t'), \\ K_{21} &= \left( \frac{\partial^2 G_-(\bar{r}_-, \bar{r}')}{\partial n \partial n'} + \frac{1}{\kappa} \frac{\partial^2 G_+(\bar{r}_+, \bar{r}')}{\partial n \partial n'} \right) \xi(t'), \\ K_{22} &= - \left( \frac{\partial G_-(\bar{r}_-, \bar{r}')}{\partial n} + \frac{\partial G_+(\bar{r}_+, \bar{r}')}{\partial n} \right) \xi(t'), \\ b_1(t) &= -U^0(\bar{r}_-(t)), \quad b_2(t) = -\frac{\partial U^0(\bar{r}_-(t))}{\partial n}, \\ \tilde{K}_{11} &= -\frac{1}{2} \left( \frac{\partial G_-(\bar{r}_-, \bar{r}')}{\partial n'} - \frac{\partial G_+(\bar{r}_+, \bar{r}')}{\partial n'} \right) \xi(t'), \\ \tilde{K}_{12} &= \frac{1}{2} (G_-(\bar{r}_-, \bar{r}') - \kappa G_+(\bar{r}_+, \bar{r}')) \xi(t'), \\ \tilde{K}_{21} &= -\frac{1}{1 + \kappa} \left( \frac{\partial^2 G_-(\bar{r}_-, \bar{r}')}{\partial n \partial n'} - \frac{\partial^2 G_+(\bar{r}_+, \bar{r}')}{\partial n \partial n'} \right) \xi(t'), \\ \tilde{K}_{22} &= \frac{1}{1 + \kappa} \left( \frac{\partial G_-(\bar{r}_-, \bar{r}')}{\partial n} - \kappa \frac{\partial G_+(\bar{r}_+, \bar{r}')}{\partial n} \right) \xi(t'), \\ \tilde{b}_1(t) &= \frac{1}{2} U^0(\bar{r}_-(t)), \quad \tilde{b}_2(t) = \frac{1}{1 + \kappa} \frac{\partial U^0(\bar{r}_-(t))}{\partial n}. \end{aligned} \quad (10)$$

The point in (9) means the derivative with respect to  $t$ . Next, we represent unknown functions  $I_{1,2}(t')$  in the form of sums

$$I_q(t') \cong \sum_{n=1}^N c_n^q \Phi_n(t'), \quad q = 1, 2, \quad (11)$$

where  $\Phi_n(t')$  are pulse functions

$$\Phi_n(t') = \begin{cases} 1, & t \in [t_n - \Delta/2, t_n + \Delta/2], \\ 0, & t \notin [t_n - \Delta/2, t_n + \Delta/2]. \end{cases} \quad (12)$$

Here,  $t_n = \frac{t_{\max}}{N} \left( n - \frac{1}{2} \right)$ ,  $n = \overline{1, N}$ ,  $\Delta = t_{\max}/N$  is the grid step, and  $N$  is the number of basis functions. Next, substituting (11) into systems of integral equations (7) and (8) and equating the left- and right-parts in the chosen on curves  $S_8^\pm$  collocation points with coordinates  $(x(t_n), y(t_n))$ , we obtain the following systems of algebraic equations in quantities  $c_n^q$ :

$$\begin{aligned} \sum_{n=1}^N (K_{mn}^{11} c_n^1 + K_{mn}^{12} c_n^2) &= b_m^1, \\ \sum_{n=1}^N (K_{mn}^{21} c_n^1 + K_{mn}^{22} c_n^2) &= b_m^2, \quad m = \overline{1, N}, \end{aligned} \quad (13)$$

or

$$\begin{aligned} c_m^1 + \sum_{n=1}^N (\tilde{K}_{mn}^{11} c_n^1 + \tilde{K}_{mn}^{12} c_n^2) &= \tilde{b}_m^1, \\ c_m^2 + \sum_{n=1}^N (\tilde{K}_{mn}^{21} c_n^1 + \tilde{K}_{mn}^{22} c_n^2) &= \tilde{b}_m^2, \quad m = \overline{1, N}, \end{aligned} \quad (14)$$

where the matrix elements and right-hand sides are calculated by the formulas

$$K_{mn}^{pq} = \int_{t_n - \Delta/2}^{t_n + \Delta/2} K_{pq}(t_m, t) dt, \quad b_m^p = b_p(t_m), \quad (15)$$

$$\tilde{K}_{mn}^{pq} = \int_{t_n - \Delta/2}^{t_n + \Delta/2} \tilde{K}_{pq}(t_m, t) dt, \quad \tilde{b}_m^p = \tilde{b}_p(t_m), \quad p, q = 1, 2. \quad (16)$$

Proceeding to the asymptotic form of the scattered wave field provided that  $r \rightarrow \infty$  and taking into account formulas (2), (5), (11), and (12), we obtain the following expression for the scattering pattern:

$$\begin{aligned} g(\varphi) &= \frac{i\Delta}{4} \\ &\times \sum_{n=1}^N \left( c_n^2 - c_n^1 i k_- (n'_x(t_n) \cos \varphi + n'_y(t_n) \sin \varphi) \right) \\ &\times \xi(t_n) \exp(i k_- [x'(t_n) \cos \varphi + y'(t_n) \sin \varphi]). \end{aligned} \quad (17)$$

Formulas (13)–(17) provide for two numerical algorithms based on systems of equations of the first and

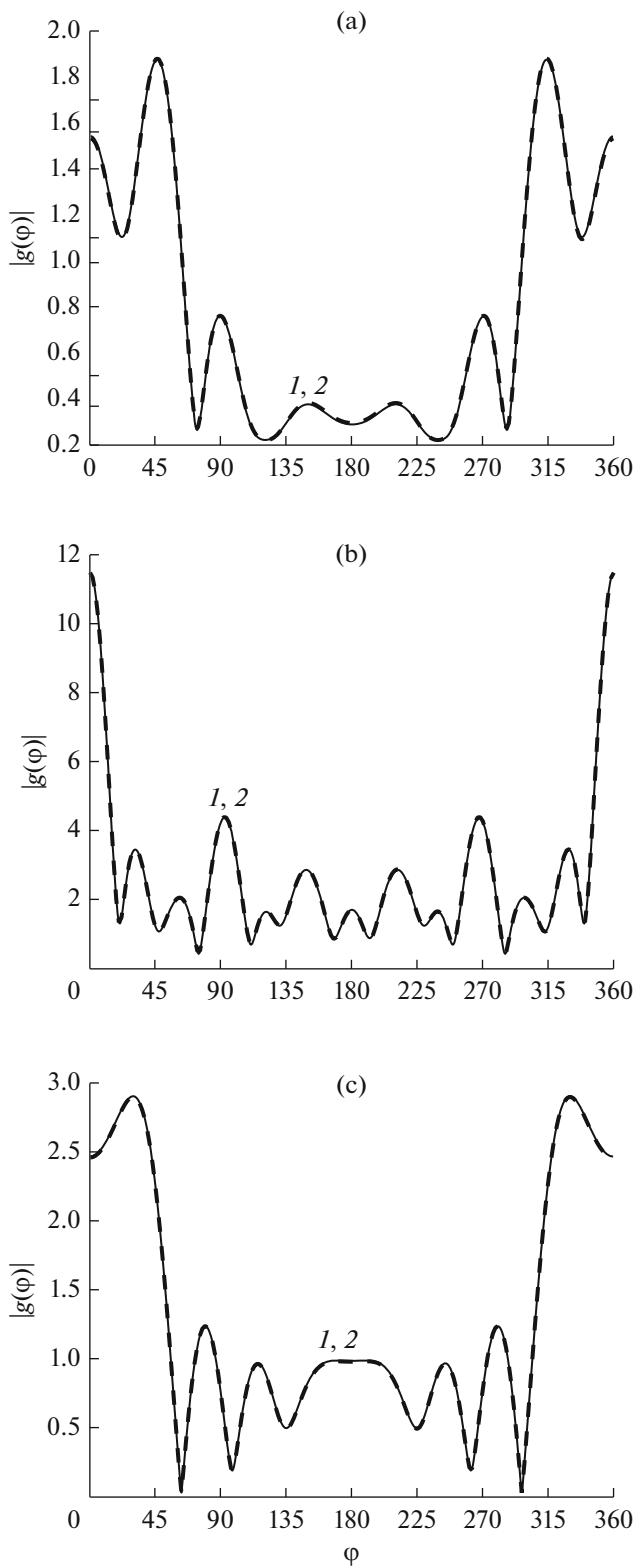


**Fig. 2.** Angular dependences of the scattering patterns of (a) the elliptical cylinder, (b) the body with the section in the form of a quatrefoil, and (c) the body with the rectangular section calculated by (curves 1) the MMDSs and (curves 2) the EBCM.

second kinds for the solution of the formulated diffraction problem.

Let a body be irradiated by the plane wave

$$U^0(\vec{r}) = \exp(-ikr \cos(\varphi - \varphi_0)), \quad (18)$$

where  $\varphi_0$  is the incidence angle and  $k \equiv k_-$ . Then, in the case, when the particle orientation with respect to irradiation angles  $\varphi_0$  is equiprobable, we obtain for the averaged pattern at the fixed angles of incidence and observation of the plane wave

$$\langle |g(\alpha)| \rangle = \frac{1}{2\pi} \int_0^{2\pi} |g(\alpha + \varphi_0, \varphi_0)| d\varphi_0. \quad (19)$$

One of the criteria for the correctness of the obtained results is the optical theorem written in the form [11]

$$\sigma = -\text{Re}(g(\varphi = \varphi_0)), \quad (20)$$

where

$$\sigma = \frac{1}{2\pi} \int_0^{2\pi} |g(\varphi)|^2 d\varphi. \quad (21)$$

As the estimate of the accuracy of the optical theorem fulfillment, we calculate the quantity, which is the relative difference of the left- and right-hand sides in formula (20),

$$\Delta_{\text{rel}} \equiv \frac{|\sigma + \text{Re}(g(\varphi_0))|}{\sigma}. \quad (22)$$

## 2. NUMERICAL RESULTS

Consider the results of numerical modeling. We assume everywhere in what follows that a body is irradiated by plane wave (18). At first, consider as an example the problem of diffraction by an elliptical cylinder, a cylinder with the section in the form of a quatrefoil, and a cylinder having a rectangular section. The equation of the contour of the body with the section in the form of a quatrefoil has the following form in the polar coordinates:

$$r = a(1 + \tau \cos 4\varphi), \quad 0 < \tau < 1. \quad (23)$$

Figures 2a–2c show the angular dependences of the scattering pattern for the corresponding geometries. These dependences are obtained for the following values of the problem parameters:  $k\delta = 10^{-4}$ ,  $\varphi_0 = 0$ ,  $\mu_i = 1$ , and  $\varepsilon_i = 4$ . The material parameters of the external medium are everywhere  $\mu_e = 1$  and  $\varepsilon_e = 1$ . The dimensions of the bodies are as follows: the ellipse semi-axes or half-lengths of the rectangular sides are  $ka = 5$  and  $kb = 1$  and the parameters  $ka = 5$  and  $\tau = 0.5$  are for the body with the quatrefoil section. The results are compared with the patterns obtained with the help of the modified method of discrete sources (MMDSs) [5, 12]. Note that the MMDSs cannot be directly applied to the problem of diffrac-

**Table 1.** Absolute and relative errors of the calculation of the scattering pattern obtained with the help of the MMDs and EBCM

$N$	SIEs of the first kind		SIEs of the second kind	
	absolute error	relative error, %	absolute error	relative error, %
Diffraction by the elliptic cylinder				
48	$1.295 \times 10^{-2}$	2.038	$1.453 \times 10^{-1}$	24.297
96	$1.904 \times 10^{-3}$	0.230	$4.183 \times 10^{-2}$	7.238
192	$6.096 \times 10^{-4}$	0.067	$1.144 \times 10^{-2}$	2.003
288	$5.834 \times 10^{-4}$	0.075	$5.539 \times 10^{-3}$	0.977
384	$5.607 \times 10^{-4}$	0.075	$3.450 \times 10^{-3}$	0.612
Diffraction by the body with the section in the form of a quatrefoil				
48	$1.643 \times 10^{-1}$	10.411	$3.836 \times 10^{-1}$	21.169
96	$2.499 \times 10^{-2}$	1.442	$9.462 \times 10^{-2}$	5.125
192	$5.802 \times 10^{-3}$	0.325	$2.534 \times 10^{-2}$	1.370
288	$2.984 \times 10^{-3}$	0.166	$1.143 \times 10^{-2}$	0.619
384	$2.176 \times 10^{-3}$	0.121	$6.474 \times 10^{-3}$	0.351
Diffraction by the body with the rectangular section				
48	$3.498 \times 10^{-2}$	4.781	$5.035 \times 10^{-2}$	6.795
96	$1.466 \times 10^{-2}$	1.956	$1.417 \times 10^{-2}$	1.715
192	$7.358 \times 10^{-3}$	0.879	$4.773 \times 10^{-3}$	0.466
288	$5.229 \times 10^{-3}$	0.561	$3.122 \times 10^{-3}$	0.248
384	$4.219 \times 10^{-3}$	0.429	$2.641 \times 10^{-3}$	0.208

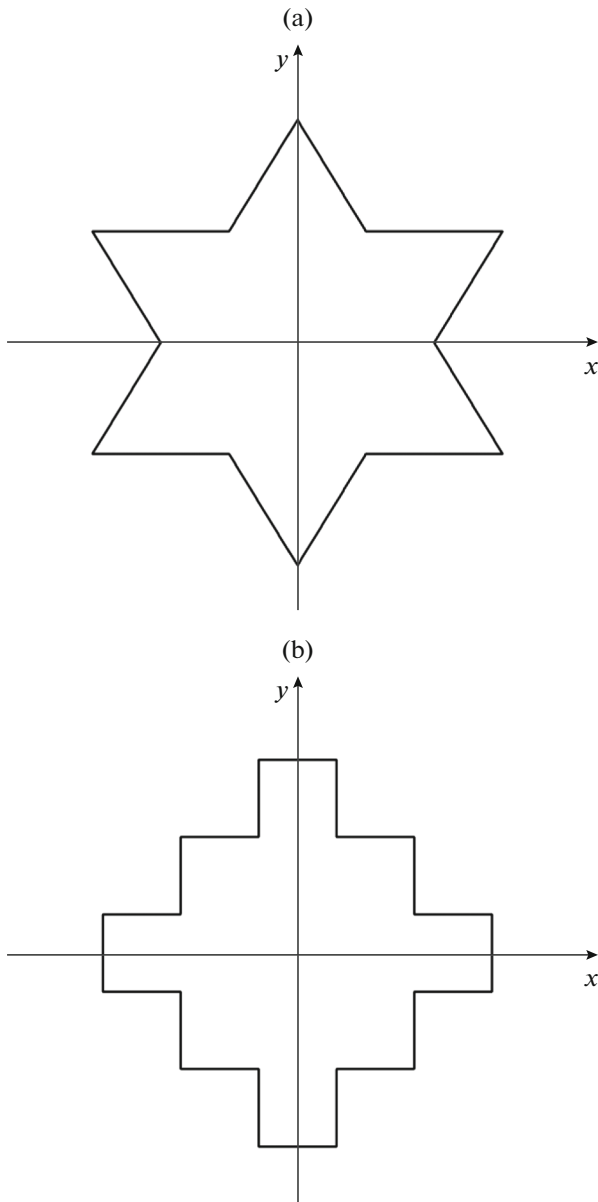
tion by bodies with boundary kinks. Therefore, the contour of the body axial section is approximated by a smooth contour [12] for the solution of the problem with the use of the MMDs. We should also note that the MMDs provides for the high accuracy of calculation for bodies with smooth boundaries, such as an ellipse, a multifoil, etc.

Table 1 shows the differences of the absolute value of the scattering pattern for the indicated geometries. These differences are obtained using two methods; the MMDs and EBCM. It is seen from Table 1 that the difference of results decreases, when the number of the used basis functions increases. The mentioned information also implies that, because of the faster convergence, the use of the equations of the first kind is more preferable for bodies with smooth boundaries. The use of the equations of the second kind provides for better results in the case of the body with the rectangular section.

Figure 3 shows the geometries of cylinders similar to fractals that have the sections in the form of the Koch snowflake and the Sierpinski curve (the first

iteration) [13]. Figures 4a and 4b illustrate the angular dependences of the scattering pattern for the indicated cylinders for the following problem parameters:  $k\delta = 10^{-4}$ ,  $\mu_i = 1$ , and  $\varepsilon_i = 4$ . The maximum transverse dimension of the body with the section in the form of the Koch snowflake and the body having its section in the form of the Sierpinski curve is  $kd = 10$  along the  $x$  axis. The two different incidence angles  $\varphi_0 = 0$  and  $45^\circ$  are considered. It follows from the figures that, for the investigated geometries, the points of the maxima of the angular dependences of the scattering pattern approximately coincide with the incidence angles of the plane wave. It is also seen that the pattern dependence for both the body with the section in the form of the Koch snowflake and the body with the section in the form of the Sierpinski curve has sufficiently large side lobes.

The accuracy of the fulfillment of the optical theorem is also controlled for the scatterer geometries considered above. In all of the cases, we choose the number of basis functions so that the number of collocation points on one wavelength is  $N_\lambda = 25$ . In this case, rel-



**Fig. 3.** Geometries of the bodies with the section in the form of (a) the Koch snowflake and (b) the Sierpinski curve.

ative permittivity  $\epsilon_i$  of the body medium is varied within the limits  $4-10^3$  and the relative permeability is chosen to be equal to unity. As the result of calculations, we obtain that the relative difference of the right- and left-hand sides of equality (20), i.e., quantity  $\Delta_{rel}$ , is small and does not exceed  $5 \times 10^{-3}$ .

We also verify the accuracy of the fulfillment of the Ufimtsev theorem [14] for the considered bodies. According to this theorem, the integral scattering cross section of a black body is exactly twice as small as the integral cross section of the perfectly conducting body with the same shady contour, i.e., the boundary

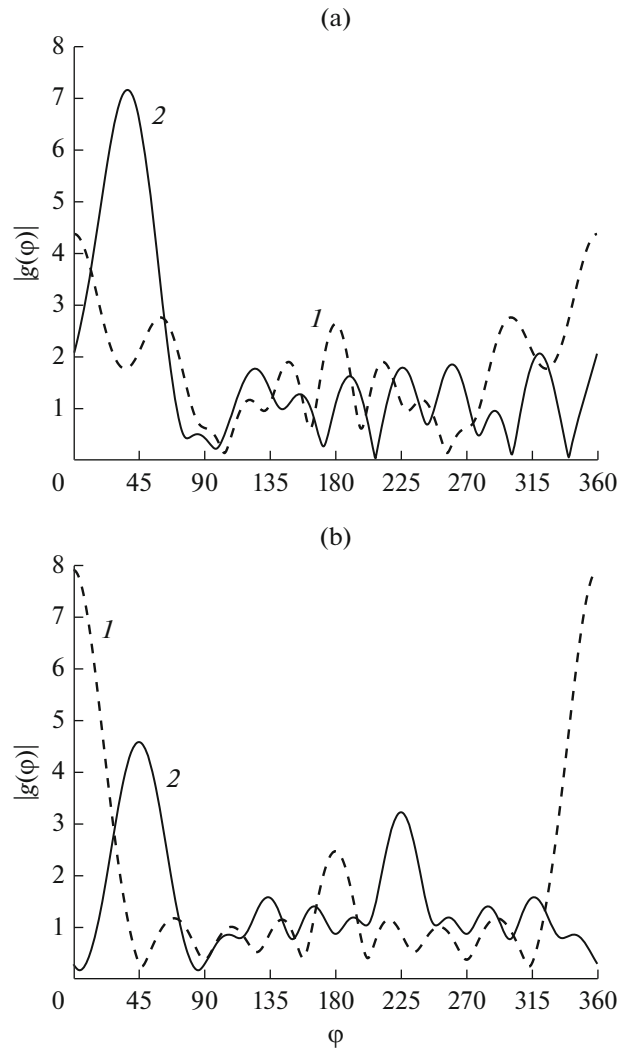


**Fig. 4.** Angular dependences of the scattering patterns of the bodies with the section in the form of (a) the Koch snowflake and (b) the Sierpinski curve for two angles: (curves 1)  $\varphi_0 = 0$  and (curves 2)  $45^\circ$ .

between the illuminated and shady parts of the body. This statement is true for all convex bodies that have the linear dimensions and minimal curvature radius much larger than the wavelength. We should note that the accuracy of the Ufimtsev theorem fulfillment depending on the scatterer dimensions is calculated in works [15, 16]. Bodies of the following geometries are considered: a spheroid, a circular cylinder, and a cone-sphere, i.e., a cone having a foundation in the form of a hemisphere. It is determined that the accuracy of the theorem fulfillment is sufficiently high, when the radius of the foundation of the considered bodies of revolution is  $ka > 4$ . For the spheroid,  $ka$  is the wave dimension of the minor semiaxis. It is interesting to find out the accuracy, within which this theorem is fulfilled for bodies having a complex geometry. Table 2 shows the results of the test of the Ufimtsev theorem for the

**Table 2.** Result of testing the Ufimtsev theorem

Scatterer geometry	Integral scattering cross section of a perfectly conducting body	Integral scattering cross section of a black body	Ratio of the cross sections
Ellipse	2.406448	1.088509	2.210774
Quatrefoil	7.876322	3.651952	2.156743
Quadrilateral	2.716768	1.251197	2.171335
Hexagon	5.928531	2.934776	2.020096
First iteration of the Koch snowflake	5.398117	2.612487	2.066275
First iteration of the Sierpinski curve	5.402070	2.498518	2.162109

scatterers of the considered above geometries. It is seen from the table that the Ufimtsev theorem is fulfilled approximately only for the bodies having the section in the form of the Koch snowflake or a hexagon.

Figure 5 shows the scattering patterns averaged over orientation angles for the body geometries considered above. It is seen from the figure that the maxima of all of the dependences correspond to angle  $\alpha$  equal to zero. It is also seen that, in the cases of the bodies with the sections in the form of the Sierpinski curve, a hexagon, and the Koch snowflake, the averaged patterns have larger values for angles  $\alpha$  exceeding  $90^\circ$  than the corresponding patterns for the elliptical and rectangular cylinders.

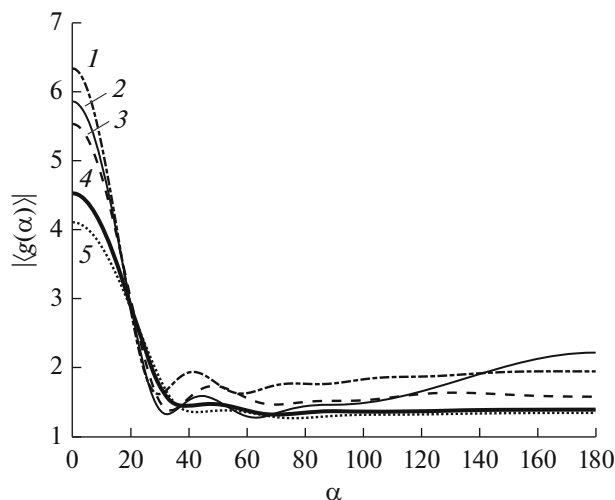


**Fig. 5.** Scattering patterns averaged over orientation angles and depending on angle  $\alpha$ : for (curve 1) the body with the section in the form of the regular hexagon, (curve 2) the body with the section in the form of the Koch snowflake, (curve 3) the body with the section in the form of the Sierpinski curve, (curve 4) the cylinder with the rectangular section, and (curve 5) the elliptical cylinder.

## CONCLUSIONS

Two numerical algorithms based on the SIEs of the first and second kinds have been developed with the use of the EBCM. These algorithms allow us to calculate the scattering characteristics of magnetodielectric bodies having arbitrary geometries. The results of calculation of the scattering pattern have been obtained for a large set of bodies of different geometries including scatterers similar to fractals. The results obtained with the help of the methods based on the EBCM have been compared with the results obtained with the help of the MMDSe. It has been shown that the EBCM enables one to obtain the results of calculation of the scattering pattern with a sufficiently high accuracy. It has been illustrated that the method based on equations of the first kind allows us to obtain results with a higher accuracy in the case of the smooth boundary of a body. The accuracy of the fulfillment of the optical theorem has been tested for the considered geometries. It has been shown that the accuracy of the fulfillment of the optical theorem is  $5 \times 10^{-3}$ . The angular dependences of the averaged scattering pattern have been obtained for different geometries of scatterers.

## FUNDING

This study was supported in part by the Russian Foundation for Basic Research, projects nos. 18-02-00961 and 19-02-00654.

## REFERENCES

1. C. F. Bohren and D. R. Huffman, *Absorption and Scattering of Light by Small Particles* (Wiley, 1983; Mir, Moscow, 1986).
2. L. N. Zakhar'ev and A. A. Lemanskii, *Diffusion of Waves Black Bodies* (Sovetskoe Radio, Moscow, 1972) [in Russian].

3. M. I. Mishchenko, N. T. Zakharova, N. G. Khlebtsov, et al., *J. Quant. Spectrosc. Radiat. Transfer* **202**, 240 (2017).
4. P. C. Waterman, *Proc. IEEE* **53**, 805 (1965).
5. A. G. Kyurkchan and N. I. Smirnova, *Mathematical Modeling in the Theory of Diffraction with Use of A-prioristic Information on Analytical Properties of the Decision* (ID Media Publisher, Moscow, 2014) [in Russian].
6. A. G. Kyurkchan, N. I. Smirnova, and A. P. Chirkova, *J. Commun. Technol. Electron.* **60**, 247 (2015).
7. A. G. Kyurkchan and N. I. Smirnova, *J. Commun. Technol. Electron.* **62**, 502 (2017).
8. A. G. Kyurkchan, S. A. Manenkov, and N. I. Smirnova, *Opt. Spektroskop.* **126**, 466 (2019).
9. D. V. Krysanov and A. G. Kyurkchan, *T-Comm. Telecommun. & Transp.* **11** (7), 17 (2017).
10. A. G. Kyurkchan and A. P. Anyutin, *Dokl. Math.* **66**, 132 (2002).
11. E. L. Shenderov, *Emission and Scattering of Sound* (Sudostroenie, Leningrad, 1989) [in Russian].
12. A. G. Kyurkchan and S. A. Manenkov, *J. Quant. Spectrosc. Radiat. Transfer* **113**, 2368 (2012).
13. R. M. Crownover, *Introduction to Fractals and Chaos* (Jones and Bartlett, Boston, 1995; Postmarket, Moscow, 2000).
14. P. Ya. Ufimtsev, *Theory of Edge Diffraction in Electromagnetics* (BINOM. Laboratoriya Znaniy, Moscow, 2007) [in Russian].
15. A. G. Kyurkchan and D. B. Demin, *Tech. Phys.* **49**, 165 (2004).
16. A. G. Kyurkchan and D. B. Demin, *Tech. Phys.* **49**, 1218 (2004).

*Translated by I. Efimova*